

# Real-Time Deterministic Power Flow Control through Dispatch of Distributed Energy Resources

Amir Fazeli, Mark Sumner, C. Mark Johnson, Edward Christopher

This paper is a postprint of a paper submitted to and accepted for publication in *IET Generation, Transmission and Distribution* and is subject to Institution of Engineering and Technology Copyright. The copy of record is available at IET Digital Library

***Abstract*--Integration of intermittent renewable resources and mass electrification of heat and transport into the existing electricity network, with limited network asset reinforcement requires incorporation of intelligence in form of active management of flexible resources within different sections of the distribution network. A hierarchical multi-level control framework is proposed for this purpose which incorporates the appropriate optimisation and control strategies at different levels. In particular a novel deterministic control algorithm for controlling power flows at the community cell level has been developed and presented in this paper. This algorithm incorporates robustness to communication and device failure and is easily expandable to an arbitrary number of devices. The simulation results presented in this paper show that the effectiveness of the proposed control technique depends on distributed energy resources flexibility and storage capacity.**

***Index Terms*—Deterministic Control, Smart Grid Control Framework, Power Flow Management, Demand Side Management, Distributed Energy Resources**

## I. INTRODUCTION

The integration of different forms of Distributed Generation (DG) to the low voltage (LV) network is on the rise as different countries have set various targets to increase their share of renewable generation capacity. As a further challenge to future

---

This work was supported in part by the HubNet project under the EPSRC grant EP/I013636/1.

Amir Fazeli is with Alstom Grid Ltd, St Leonards Avenue, Stafford ST17 4LX, UK (e-mail: amir.fazeli@alstom.com). The other authors are with the Power Electronics, Machine and Control group at the University of Nottingham.

distribution systems, the electrification of heat and transport is also expected to occur in the near future which will result in a substantial increase in electricity demand [1]. The integration of intermittent renewable generation and electrification of heat and transport will cause the thermal and electrical limits of the distribution network assets to be exceeded. In particular the foreseen adverse effects [2] for the LV urban radial network include:

- Increased voltage drop at the consumer end of LV feeders
- Distribution transformer and feeder overloading
- Increased network losses
- Voltage unbalance
- Under-frequency
- Current harmonics

Mass integration of the aforementioned new resources to the passive distribution network, could only take place either by reinforcement of the existing network assets (which will prove prohibitively expensive particularly in urban areas) or incorporation of a certain degree of intelligence in the form of active management of flexible resources within different sections of the distribution network.

It is worth noting that this project's objective was to explore the latter option. Therefore the available literature is reviewed in search of an appropriate algorithm for regulating the power flow at the community level through controlling/scheduling the operation of the available Distributed Energy Resources (DER). An interesting review of load scheduling techniques has been presented in [3]. According to [3] the majority of load scheduling schemes are based on application of an optimisation algorithm in which the forecasted load of an aggregator is used. It is however important to note that these methods do not consider the temporal variation of load availability (a measure of the physical characteristics and availability of the load for control) and the willingness to participate in control activities. In addition to that the effectiveness of such schemes highly depends on the reliability of the forecasted load profile. Considering that the load profile cannot be forecasted accurately at a low aggregation level and within a community, the application of a direct load control technique is expected to be ineffective at this level. Therefore any algorithm used for regulating power flow within a community needs fast decision making capabilities based on the instantaneous power flow and the availability of the DERs, rather than predicted stochastic load profile of individual devices. This fast and dynamic decision making capability would allow the algorithm to dynamically adjust the connection/disconnection of the DERs to ensure effective optimisation/control of the community's power flow during the entire period. An autonomous regional active network management system (AuRA-NMS) has been presented in [4, 5] which aims to integrate different control and network management tasks including:

- Steady state voltage control

- Automatic restoration
- Power flow management
- Network optimisation strategies

The power flow management functionality of the AuRA-NMS utilizes a constrained programming approach in which the outputs from certain generators are constrained (with a pre-specified threshold) to meet the thermal rating of the network assets [5]. AuRA-NMS applies the constraint satisfaction problem only to embedded generation units; nevertheless the power flow management technique presented in this work determines the correct combination of DERs from three different DER categories comprising loads, DG and storage.

Having reviewed the available literature in this area it became apparent that the majority of the previously published research appears to be aiming at devising specific solutions for individual problems. Most of the previously reported optimisation techniques do not consider DER characteristics, and rely on the forecasted load profile. Therefore they are unlikely to result in effective control outcomes when applied at a low aggregation level. This has led the authors to propose the Community Power Flow Control algorithm (CPFC) a novel deterministic control algorithm for regulating power flow within a section of the distribution networks. CPFC has been developed by the authors for real time execution at the lowest level (i.e. community) of a hierarchical smart grid framework. This framework will be presented in a future publication. CPFC is capable of determining a suitable combination of DERs for dispatch in real time in a coordinated manner, in order to reduce the difference between the instantaneous Community Power Flow ( $CPF$ ) and the Community Power Flow Target ( $PF_T$ ). This algorithm entails real time decision making capabilities and is therefore effective at controlling the power flow within a community. In addition to that it accounts for the operation of every individual DER. To the authors' knowledge no flexible and robust deterministic control algorithm for regulating power flows at the community cell level of a hierarchical system has been published to date.

## II. DEVELOPED MODELS

Before explaining the logic behind the CPFC algorithm it is worth mentioning that the development of this algorithm required modelling the operation characteristic and limitations of every participatory DER. Therefore the following stochastic DER, load and DG models have been created in Matlab/Simulink with a temporal resolution of one second:

- Domestic electricity load [6]
- Electric vehicle charging [7]
- Domestic heating load [8]
- Ground source heat pump [9]
- Photovoltaic generation [10, 11]

- Wind power generation [12, 13]
- Community battery energy storage [14]

A novel modelling technique for accurate quantification of electric vehicle charging requirements in terms of charging energy, power and duration has been developed by the authors. This EV model is comprised of the interaction of a lithium ion battery model [14] with a novel stochastic method for quantifying the vehicle's temporal journey characteristic. This modelling approach has been described in [7]. It is worth mentioning that since the majority of network optimisation and control strategies attempt to regulate active power to achieve a combination of objectives concerning generation/delivery/utilization of active power, active power flow has been chosen as the primary control parameter in the CPFC's operation. It is however important to note that since reactive power also influences the voltage levels and thermal capacity of network asset, it should be used as a control parameter. The simplest means of incorporating this is to use complex power as the control parameter in CPFC's operation. The communication requirements and the operation of the CPFC algorithm are explained in detail in the next section.

### III. POWER FLOW CONTROL WITHIN A COMMUNITY CELL

#### A. Problem introduction

The operation of the CPFC algorithm is based on determining the connection of dispatchable DERs within the community in order to reduce the difference between the instantaneous community power flow ( $CPF$ ) and a community power flow target ( $PF_T$ ) signal. This is a control problem incorporating feedback as illustrated with the block diagram shown in Fig.1.

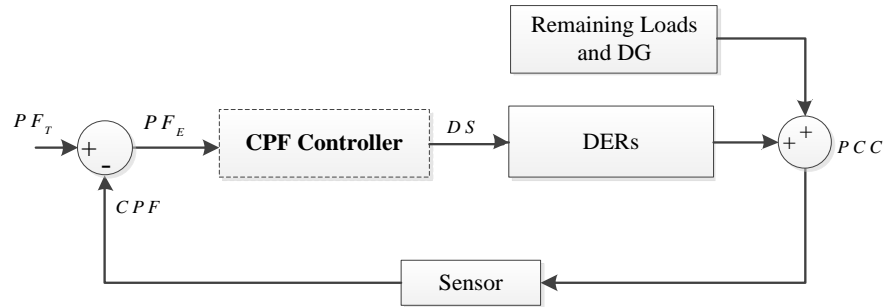


Fig.1. Community power flow controller with a negative feedback loop

The  $PF_T$  is generated at the “cluster of community cells” level of the hierarchical framework and is broadcasted to every community cell within that cluster. Real time current and voltage measurement at the point of common coupling of the community provide an instantaneous measure of the community power flow. The  $CPF$  is provided as negative feedback and is subtracted from the target value to generate the Community Power Flow Error ( $PF_E$ ) which is then fed into the  $CPF$  controller shown in the dashed box. The controller runs the CPFC algorithm to decide on connection/disconnection of the required number of DERs and effectively generates a unique dispatch signal (DS) for every participatory DER at its outputs. Real time dispatch of

these flexible DERs is the corrective control measure which effectively forces the instantaneous  $CPF$  to match its reference value  $PF_T$ . It is worth noting that selecting an appropriate  $PF_T$  magnitude is crucial to CPFC's operation and the resultant control actions. Selecting a relatively low value of  $PF_T$  causes simultaneous disconnection of devices which in turn results in their concurrent reconnection and re-emergence of undesirable peaks greater than the original power flow waveform. On the other hand setting a relatively high value of  $PF_T$  could result in sporadic device disconnection and underutilization of the available capacity. In the proposed control framework this signal is expected to come from the intermediate level of cluster of community cells as an outcome of a heuristic optimisation algorithm, the determination of which is set as future work from this project. Nevertheless for the purpose of developing the CPFC a simpler approach is taken for determination of  $PF_T$  in which the average power of a single dwelling has been calculated (i.e. considering different DER penetrations) and scaled with respect to the community size to derive a constant  $PF_T$  value. In this study, DER dispatch refers to either connection disconnection or enforced-connection operations of loads, DG, and storage units. The difference between these three DER operation modes is explained below.

### *B. System Communication Requirements*

Before the structure of CPFC's dispatch functions are explained it is prerequisite to understand and distinguish between the two distinct classes of signals exchanged between every DER and the central  $CPF$  controller that runs the CPFC. These signals are termed the "DER Status" and the "DER Dispatch" signals. The DER status signals are monitoring signals which determine the status of every DER for dispatch. They comprise the "DER connection request" and the "DER enforced-connection request", logic signals that are broadcasted to CPFC and used in its decision making.

#### *1) DER connection request signal*

Every DER needs to inform the CPFC about its instantaneous mode of operation. For instance if the DER is a DG unit, capable of generating a certain amount of active power, then that DER would be requesting connection from the CPFC to deliver its potential generation. Similarly if the DER is a GSHP, it would be requesting connection based on the output of the hysteresis which regulates the temperature of its thermal storage. An EV would be requesting connection if it is plugged in to a charging point at a dwelling and not fully charged. All DERs considered in this study generate a connection request signal which is broadcast to the central  $CPF$  controller where it is used in the CPFC's dispatch functions.

#### *2) DER enforced-connection request signal*

As two of the loads considered in this study inherently employ a thermal storage element (i.e. refrigerator and GSHP) it is possible to make full utilization of their thermal storage by operating them in "shedding" or in "enforced-connection" modes.

Either the “shedding” or “enforced-connection” operation can occur provided that the load has been selected for this type of operation mode by the CPFC and its maximum shed/enforced-connection condition has not been reached. It is necessary to define and use the maximum shedding/enforced-connection limits in order to avoid any prolonged shed or enforced-connection which could result in unrealistic temperature values for such loads. It is possible to use the conventional hysteresis band for these limits. However this confines such modes of operation within the conventional hysteresis band with a lower available thermal storage capacity. Therefore in order to increase the available thermal storage capacity of these loads two additional designated hysteresis bands are created and used to regulate the internal temperature of the thermal storage element of such loads during shedding and enforced-connection operation modes. This is illustrated later in the paper in Fig.5 which shows how three status signals (each with Boolean format) are generated from such hysteresis controllers for a GSHP hot water storage tank. These signals are then broadcasted to the community’s central *CPF* controller where they are used in CPFC’s decision making. A similar shedding limitation mechanism has been devised for other loads, to avoid their prolonged load shedding, taking into account any limitation that the user may wish to specify. For instance a reconnection request signal has been created for EVs which responds to shedding time (rather than temperature in case of thermal load). This ensures that the EV is not continuously shed longer than a certain period specified by the user. Upon receiving the DER status signals the CPFC runs and determines a set of dispatch signals (i.e. one for every DER). The dispatch signals are fed back to every individual DER to facilitate their connection/disconnection and this closes the feedback loop in this system.

### C. Deterministic Power Flow Control Algorithm

The central *CPF* controller receives the DER status signals and uses them in the CPFC’s algorithm for determining the right number of DERs for dispatch. The CPFC’s operation is based on the sequential execution of a set of sub-functions contained in the “*CPF* Reduction” and the “*CPF* Increase” functions as shown on the left and right hand side of Fig.2 respectively. Only one of these two functions is executed at any time depending on whether the *CPF* is above or below its target value  $PF_T$ . During every time step the values of  $d$  starts from 0 and continues to increment. With every incrementation of  $d$  a new DER is dispatched. This process is continued until the *CPF* reaches its target value. An example of the CPFC source code for a community of 100 dwellings, with DG and EV resources has been provided in Appendix A for illustration purposes. This source code is written in C programming language and is executable in SIMULINK s-function block [15].

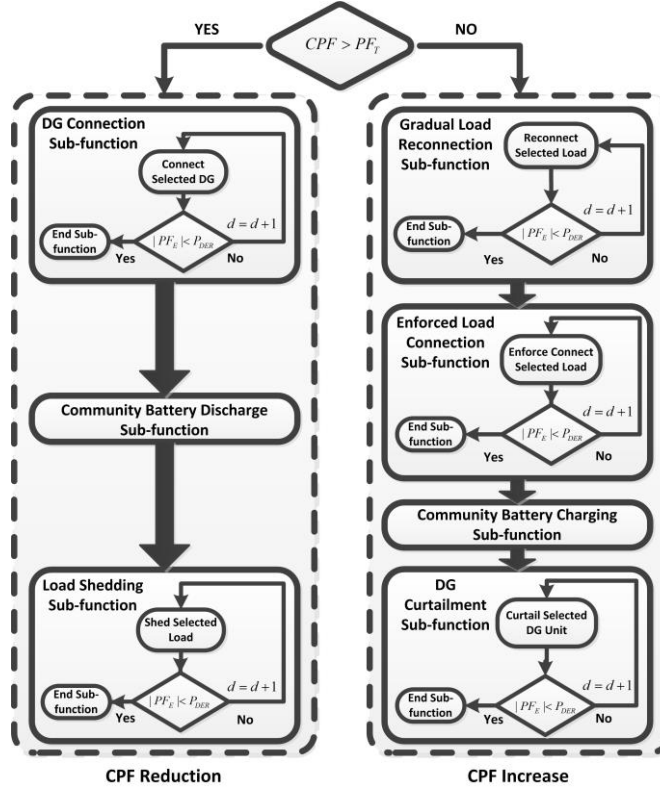


Fig.2.The structure of the CPFC's dispatch sub-functions

Dispatch coordination takes place during execution of every sub-function to maintain an even DER participation in every group. Coordination occurs between participatory DERs in every sub-function to ensure selection of DERs which have been dispatched the least during previous time steps. This is carried out using a sorting subroutine (as evident in the sort code) which rearranges the order that DERs are selected for dispatch according to their overall dispatch count. Coordination at every time step could result in continuous switching of different DERs (which could be owned by different customers). In order to avoid this effect, it is best to perform coordination at a relatively lower speed (10 minutes interval used in this case).

### 1) Community Power Flow Reduction Function

The “*CPF* Reduction function” is executed to reduce the *CPF* when its magnitude is greater than the target value  $PF_T$ . This function is comprised of the “distributed generation connection sub-function”, the “storage discharge sub-function” and the “load shedding sub-function”. These sub-functions are executed sequentially until the adequate combination of DERs for reducing *CPF* close to  $PF_T$  is found. Every DER is identified by their index  $d$ , as shown in Fig.2. The immediate measure for reducing *CPF* is connection of any on-site distributed generation that is requesting connection. Therefore the DG connection sub-function has been assigned execution priority. The community battery starts to discharge upon termination of the DG connection sub-function provided that *CPF* still remains above its target value, and the battery is requesting to discharge. The tertiary measure of reducing *CPF* close to its target is disconnection of loads that are requesting connection. A sequential shedding order is followed

for the three load groups starting with shedding EVs followed by GSHPs and refrigerators, aiming to shed the most essential loads last. Loads stop participating in the algorithm when they start to request reconnection (i.e. maximum shedding period is reached).

## 2) *Community Power Flow Increase Function*

The “*CPF Increase*” function has the opposite role to its counterpart and is only executed to increase the *CPF* when it is below its target value  $PF_T$ . This function is comprised of the “gradual and enforce load connection sub-functions”, the “storage charging sub-function” and the “generation curtailment sub-function”. These sub-functions are executed sequentially until a suitable combination and adequate number of DERs for increasing the *CPF* close to  $PF_T$  is found. The immediate measure for increasing *CPF* is gradual reconnection of loads that were selected for shedding and are still requesting connection. A sequential reconnection order is followed (i.e. opposite to shedding order) starting with refrigerators, followed by GSHPs and, EVs aiming to reconnect the most essential loads first. Such loads are gradually reconnected until they stop requesting connection. The secondary measure for increasing *CPF* is to enforce connect loads that are not requesting connection. In case of thermal loads this effectively makes optimum use of their thermal store as the stored heat is increased (or charging EV battery if *vehicle to grid* was considered). GSHPs are given enforced-connection priority over refrigerators considering that they have a larger storage capacity and are less essential to the user. The tertiary action for increasing *CPF* close to its target value is charging the community battery (i.e. either from the grid or excess DG) provided that the battery is requesting connection (i.e. determined according to its SOC). This could only occur following termination of load reconnection and enforce-connection sub-functions provided that *CPF* still remains below its target value. The quaternary measure of increasing *CPF* close to its target is disconnection of distributed generation that are requesting connection. This resembles a situation when the grid can’t accept excess distributed generation due to voltage rise within a section of the network.

## D. *CPFC’s Features*

In addition to the CPFC’s ability to determine the adequate number of DERs to dispatch in a coordinated manner within a community, this novel algorithm displays the following features:



1) *Robustness* - The CPFC algorithm has minimal reliance on communication and is robust to communication failure and interruption in the DER operation.

2) *Scalability* - Since the CPFC has a bottom up structure and relies on limited communication it is easily expandable.

3) *Maintaining power flow stability* - The CPFC has been designed to ensure system stability and proper CPF corrective control action avoiding any CPF oscillation around its reference value  $PF_T$ . This is enabled by reverting DER dispatch if it causes CPF to cross over  $PF_T$ .

4) *User interface and override function* - A simplistic user override function has been incorporated to allow the user to withdraw their DER from the CPFC's operation.

#### IV. RESULTS AND ANALYSIS

Fig.3. shows the effect of running the CPFC in real time to control the CPF for a community of 100 dwellings with 60% EV penetration (i.e. 6.6kW charging power, 24kWh battery capacity [16]), 50% GSHP penetration (i.e. 2.16kW load power [17]), 50% PV (with connection to the mains network) and 100% refrigerator penetration. The simulation time for this particular community was just over 15 minutes (i.e. on a computer with 3.2GHz CPU and 32GB of RAM). As evident in Fig.3 – Fig.8 a simulation period of 1 day and 9 hours has been chosen. The reason for selecting this simulation period is due to the fact that the late evening hours and the early morning hours are inherently two distinct periods in terms of power and excess energy levels. Therefore it is necessary to examine the effectiveness of the CPFC algorithm during these periods in a continuous simulation.

### Community Power Flow with and without Control

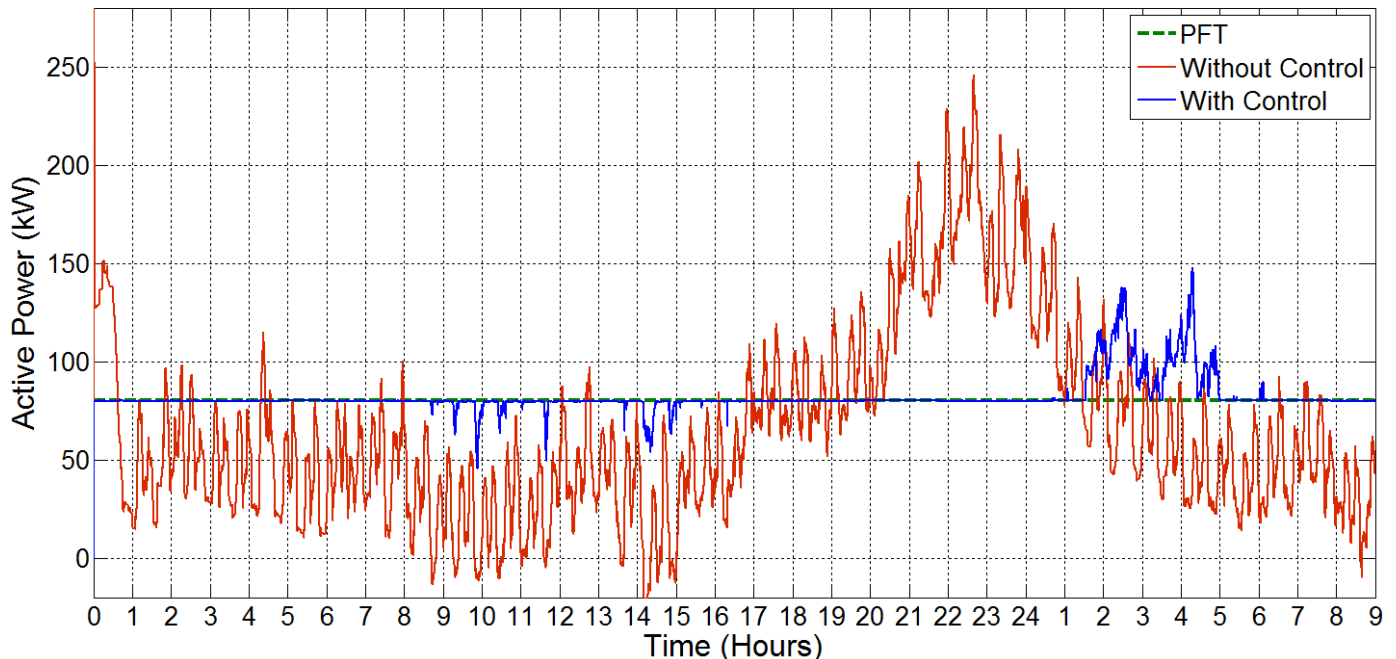


Fig.3. Community power flow with and without the CPFC (only DG and load dispatch)

The community battery has been omitted in this simulation in order to merely study the effect of execution of the load and DG

sub-functions. The CPFC effectively finds and dispatches the correct number of DERs, (making sure that the least previously dispatched devices are selected at every instant) in order to control  $CPF$  with respect to its target value.

It is worth noting that connection of DG could increase/decrease the current flows in the LV feeders, depending on the location and size of the unit. However this aspect has not been considered in this study and is left for future work. It is also important to note that in this model the maximum shedding period of EVs (i.e. as explained in section III) was selected to be between 4 to 6 hours. Every GSHP has been allocated a hot water storage tank of 200 litres which has an equivalent 1.7 kWh of electrical storage capacity, as quantified using “(1)”.

$$E = \frac{2.78 \times 10^{-7} \times C_p \times M \times \Delta T}{COP_A} \quad (1)$$

$\Delta T$  Is the overall hysteresis width used to regulate the temperature of GSHP hot water tank.  $C_p$  is the specific heat capacity of water and  $M$  is the overall mass of water in the storage tank. The value of  $C_p$  was obtained from [18] as 4.186 joule/gram °C. 200 liters of water has an equivalent mass of 200 Kg.  $COP_A$  is the average value of GSHP’s coefficient of performance across a day obtained from simulation. In this particular simulation the load and DG groups of dispatch sub-functions shown in Fig.2 have been executed and this results in an average  $CPF$  reduction of 82.6% when it is above and a  $CPF$  increase of 98.3% when it is below the  $PF_T$ . Load factor is a measure of the average power over peak power during a given period and load loss factor is a measure of losses incurred as a result of peak power. These two parameters are quantified using “(2)” and “(3)” respectively for an entire day. Since the simulation window considered in this study was 24 hours, the upper limit of summation elements in (2) and (3) and the division factor in the numerator of these equations corresponds to 86400 second in that simulation period. Applying  $CPF$  control results in the value of the load factor to increase from 0.36 to 0.76. The value of the load loss factor has also risen from 0.15 to 0.43.

$$Load\ Factor = \frac{\sum_{t=1}^{86400} CPF}{86400 \cdot MAX(CPF)} \quad (2)$$

$$Load\ Loss\ Factor = \frac{\sum_{t=1}^{86400} CPF^2}{86400 \cdot MAX(CPF^2)} \quad (3)$$

As illustrated in Fig.3, the CPFC is capable of controlling the  $CPF$  close to its reference value for the majority of the time with

the exception of three intervals during which the  $CPF$  has deviated from its target value  $PF_T$ . The first two deviations from the target appear during morning and midday hours of day one. These two deviations occur when the CPFC algorithm runs out of resources to reconnect/enforce connect in order to increase  $CPF$  closer to the target. The reemergence of peaks during the interval 01:30-05:00 hours reduces further improvements to load factor and load loss factor. This deviation is primarily caused by simultaneous reconnection of EVs as they reach the end of their maximum shedding period. Fig.4 shows the aggregated GSHP load power with and without  $CPF$  control, and Fig.5 shows the temperature variation of three GSHP storage tanks. According to Fig.4 it is evident that the CPFC manages to modulate the total GSHP power for the majority of the day. The  $CPF$  modulation is also reflected on the temperature variation of three GSHP storage tanks as shown in Fig.5. For the sake of clarity only the temperature profiles of three GSHP storage tanks are shown and the remaining tank temperatures follow a similar pattern.

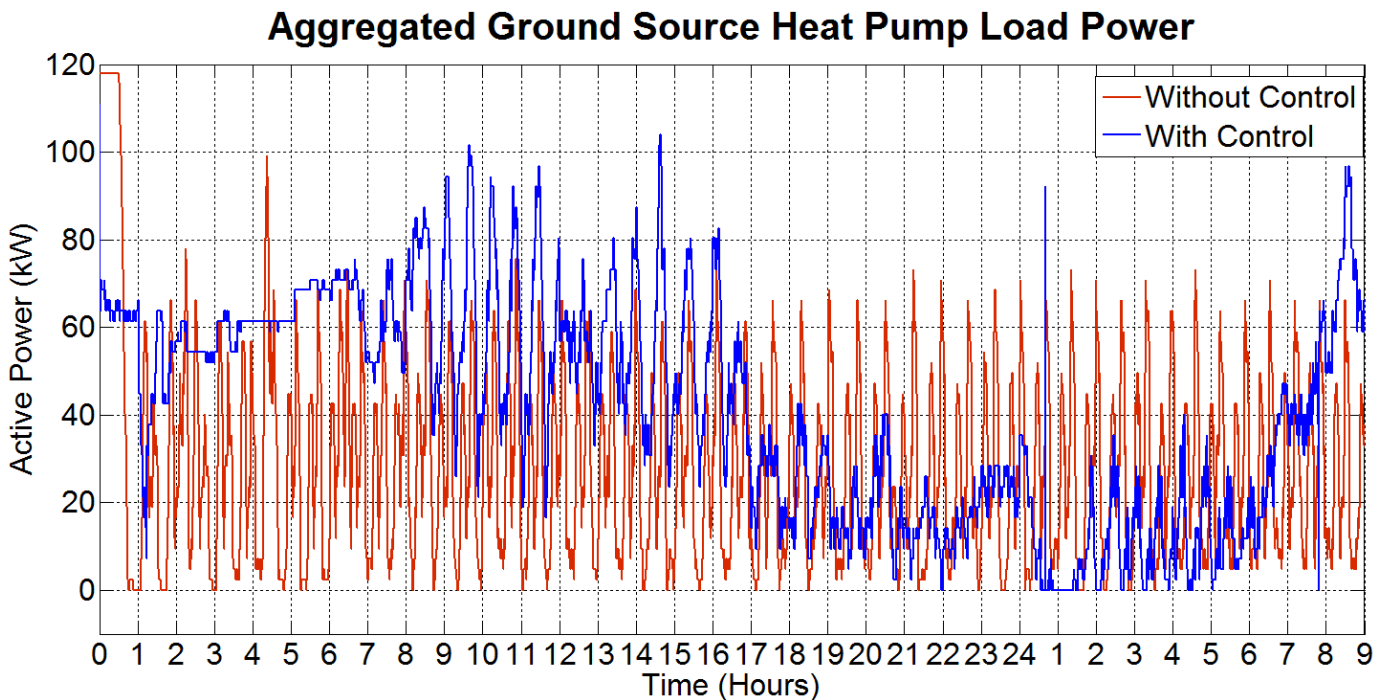


Fig.4. Total GSHP power before and after application of CPFC

The conventional hysteresis band for regulating the internal temperature of a GSHP system storage tank has been selected between  $52.5^{\circ}\text{C}$ - $57.5^{\circ}\text{C}$ . During shedding operation the tank temperature is reduced and regulated using a  $40^{\circ}\text{C}$ - $43^{\circ}\text{C}$  hysteresis band (i.e. as the GSHP is shed ) and during enforced-connection the tank temperature is increased and regulated using a  $67^{\circ}\text{C}$ - $70^{\circ}\text{C}$  hysteresis.

### Ground Source Heat Pump Storage Tank Temperature Variation

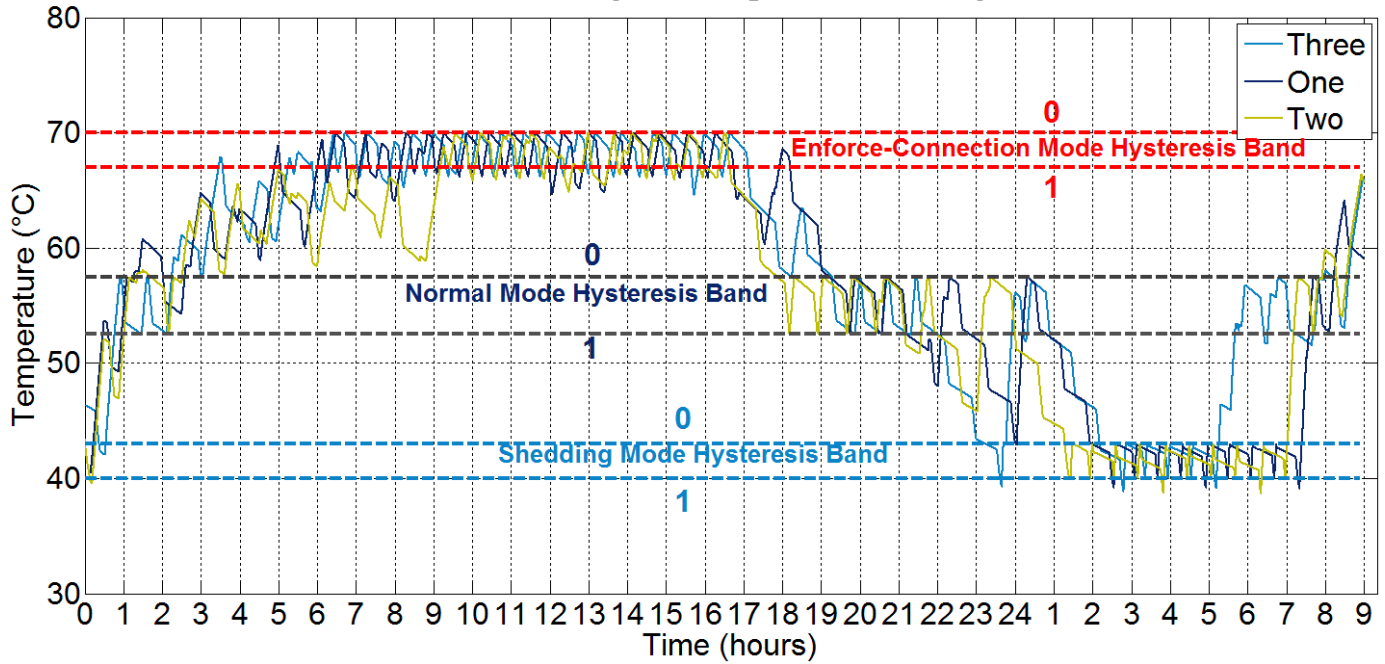


Fig.5. Dispatched GSHP storage tank temperature

The last deviation between the  $CPF$  and  $PF_r$  (between 01:30-05:00 hours) in Fig.3 is primarily due to the simultaneous reconnection of EVs as they reach the end of their maximum shedding period. This can be clarified when Fig. 4, Fig.6 and Fig.7 are compared. Fig.6 shows the aggregated EV power with and without the CPF control.

### Aggregated Electric Vehicle Load Power

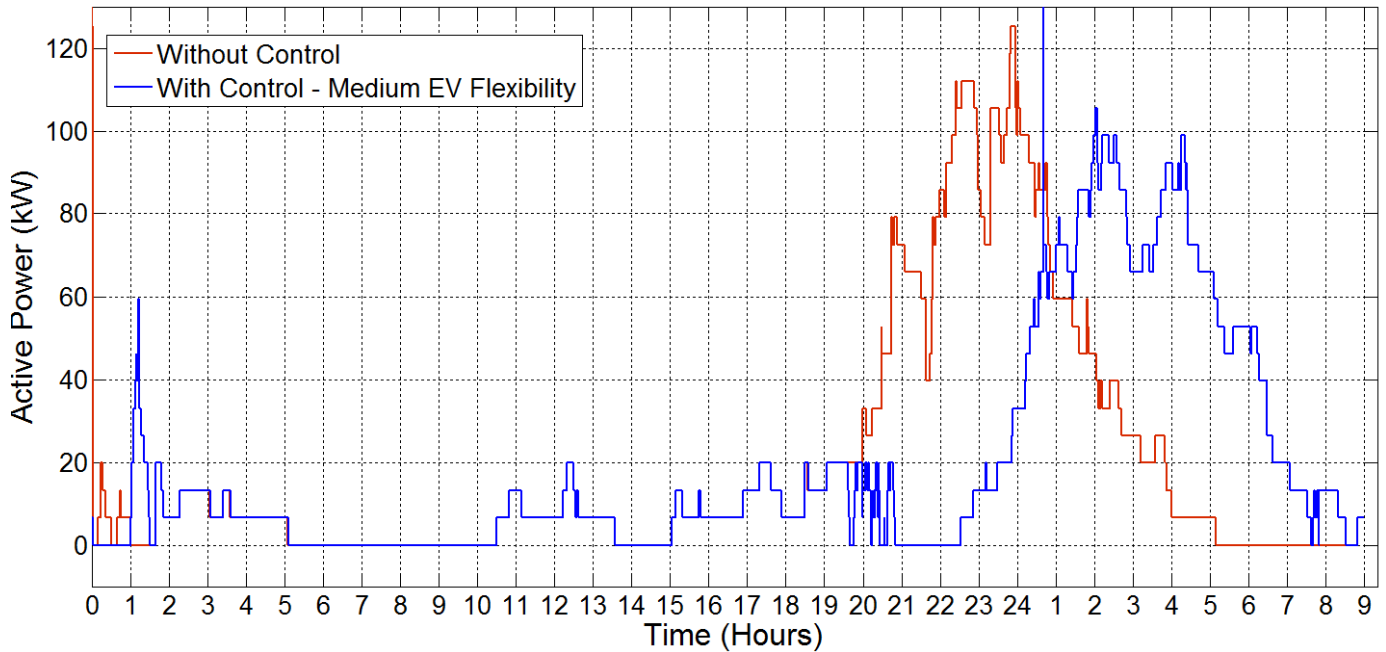


Fig.6. Total EV charging power before and after application of CPFC

Fig.7 shows the SOC variation of three EVs throughout the day. According to Fig.6 the total controlled EV charging power is

modulated effectively for majority of the day with the exception of the interval 01:30-05:00 hours during which the controlled EV charging power is nearly as much as the uncontrolled case. The CPF modulation is also reflected on Fig.7 which shows SOC variation of three EVs and their contribution towards the control action.

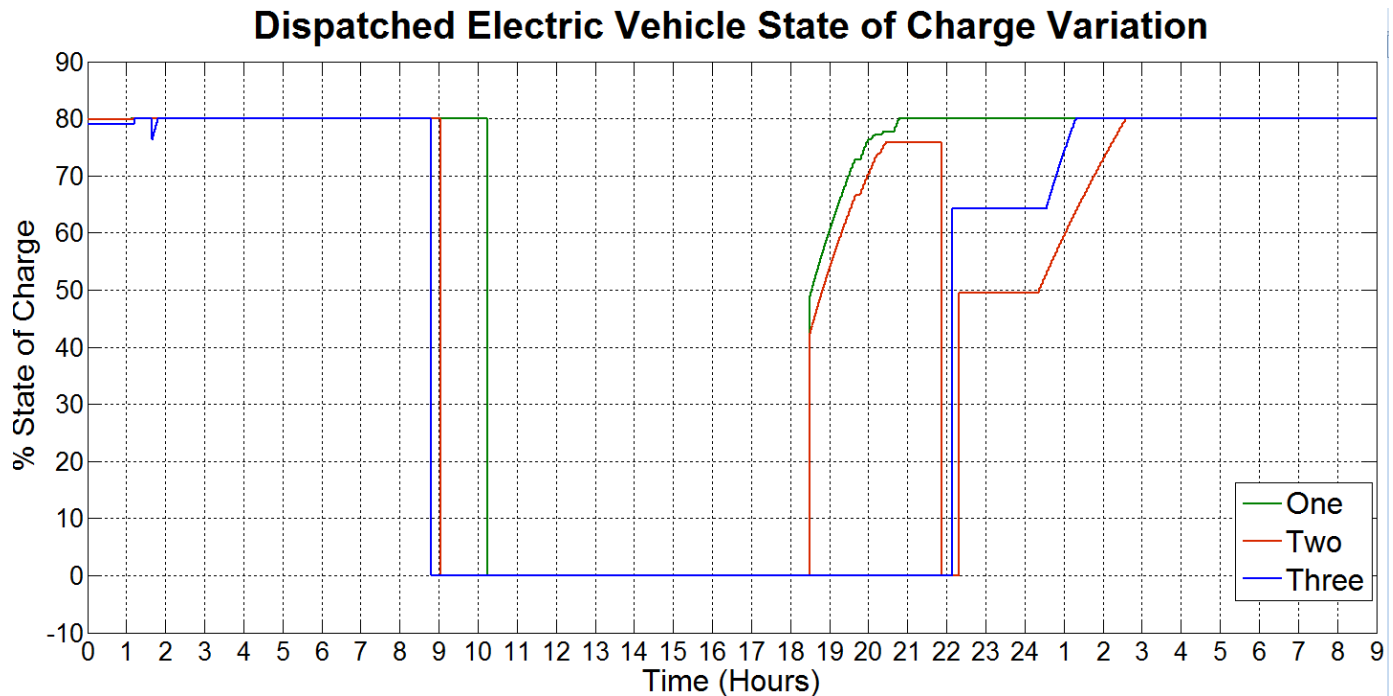


Fig.7. Dispatched EVs state of charge variation

The SOC variation shows periods when the EVs are shed (i.e. when the SOC is constant, between 15% and 80%) in addition to periods when EVs are on a journey consuming energy (i.e. SOC is zero); and durations when EVs are at the dwelling and fully charged with a SOC of 80%. In order to avoid indefinite shedding operation for any EV a maximum shedding period (at the discretion of user) has been selected for every EV. According to Fig.7 the EVs start to be shed as soon as they arrive at the dwelling from their last journey. They continue to be shed up until 01:00 hour at which point they reach the end of their maximum shedding period and start to reconnect. This causes the re-emergence of the late evening peak as observed on Fig. 3. When the magnitude of the  $PF_E$  is less than the total power available for shedding the CPFC ensures that only the required number of devices are disconnected to force the  $CPF$  to a new value very close to but still above the target. This ensures system stability as it eliminates  $CPF$  oscillation around  $PF_T$ . For instance during the interval 19:30-20:30 two EVs are requesting connection however since the magnitude of the  $PF_E$  is less than the total power available for shedding, the CPFC only sheds EV one and EV two is allowed to be charged. The remaining gap in that period between  $CPF$  and  $PF_T$  is compensated by the CPFC shedding other loads with lower power rating (e.g. fridge and GSHP). The decision for selection of the appropriate EV for disconnection is carried out through coordination. Similar to the GSHP three distinctive hysteresis bands have been defined to

regulate the internal temperature of refrigerators and are included in the CPFC's operation. Every refrigerator has a load power of 190W and according to "(1)" an equivalent electrical storage capacity of 1.2 kWh. Since refrigerators have a less storage capacity they inherently have a short time constant compared to other DERs considered in this study. Therefore their contribution towards any energy management measure is thought to be minor however they are quite effective at compensating minor *CPF* deviations from  $PF_T$ . 50% of the dwellings within this community were assigned a  $1.68 kW_p$  PV array and every one participated in the CPFC's operation. It is worth noting that setting higher values for the maximum EV shedding duration would enable the CPFC to shift the remaining late evening peak to the early hours of the next day during which there is sufficient capacity between *CPF* and  $PF_T$  to both fully charge all the EVs and ensure very effective *CPF* control. This assumption however depends on each consumer's preference and the uptake of technology which cannot be predicted with great accuracy. Incorporation of more intelligent decision making in the CPFC's selection logic process could reduce the aforementioned *CPF* deviation, and different possible approaches are recommended as future work from this project.

For example one possibility is to generate number of individual power flow error signals for every one of the CPFC's dispatch sub-functions, in order to limit the participation from different DER groups to a number of individual and optimal values. A model of a low voltage feeder supplying a community of 100 dwellings was created using the Kersting's ladder iterative technique [14]. Fig.8 shows how by controlling the instantaneous power flow the CPFC has eliminated majority of the voltage sag at the end of the feeder during the interval 17:30 -03:30 hours. However the last undesirable *CPF* deviation from  $PF_T$  has resulted in minor voltage sags below the lower statutory limit. Overall this demonstrates that despite having power flow as the control parameter feeder voltage has also been indirectly regulated.

In order to eliminate this deviation number of possible options is currently under consideration. One possibility is to use voltage at different nodes across the feeder as a secondary control parameter in the CPFC's operation.

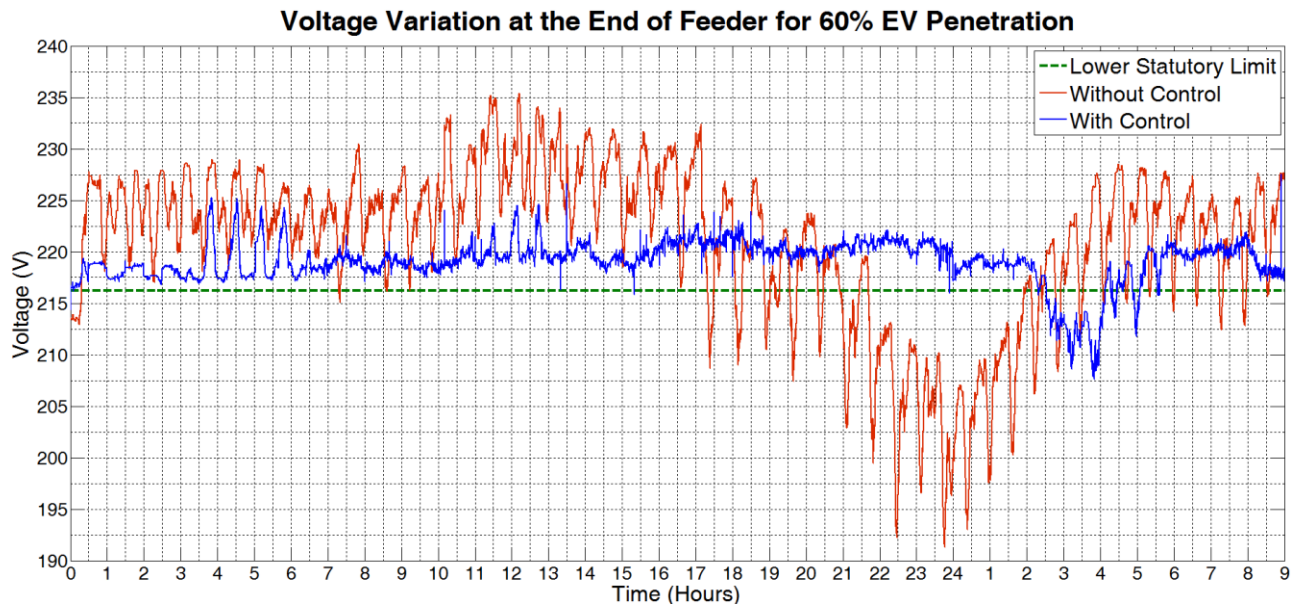


Fig.8. Influence of CPFC on feeder voltage

A more comprehensive analysis of the impact of the CPFC's operation on the LV network and any further improvements to the CPFC in this respect has been described in [19].

## V. CONCLUSION

This paper presents the operation of the CPFC algorithm for regulating the power flow at the lowest level of a hierarchical smart grid control framework. As illustrated in this paper the primary functionality of the CPFC algorithm is to determine the correct number of DERs for dispatch in a coordinated manner in order to control CPF at its target value  $PF_r$ .

In addition to the aforementioned functionalities the CPFC's robustness to communication and device failure, scalability, stable control and the appropriate user interface and override functions form the important attributes of this reliable novel control technique.

A laboratory based microgrid test facility is currently under development details of which are presented in [20]. As part of that work the CPFC has been fully rewritten in C and executed on a micro controller, both in an emulated laboratory and in an existing community.

It is important to note that DER flexibility (e.g. Maximum EV shedding duration) and storage capacity (e.g. hysteresis width and storage capacity of a GSHP storage tank) affect the control outcome and the resultant improvement to the figures of merit. Since DER flexibility and storage capacity are left to the discretion of the user they cannot be predicted with absolute certainty. Therefore it is vital to enhance the CPFC robustness and adaptability to ensure its effective operation under any DER flexibility and storage level.

With this purpose in mind different ideas are currently under investigation including incorporation of an additional functionality

in CPFC decision making to enable selection of the optimum combination of DERs for dispatch. The inclusion of vehicle to grid operation for the EVs is also expected to enhance the effectiveness of the CPFC algorithm. Therefore this option will also be considered in future work.

## VI. REFERENCES

- [1] E. E. Limited, "Electric vehicles in the UK and Republic of Ireland: Greenhouse gas emission reductions & infrastructure needs," Element Energy Limited August 2010.
- [2] P. Papadopoulos, L. M. Cipcigan, N. Jenkins, and I. Grau, "Distribution networks with Electric Vehicles," in *Universities Power Engineering Conference (UPEC), 2009 Proceedings of the 44th International*, 2009, pp. 1-5.
- [3] D. S. Callaway and I. A. Hiskens, "Achieving Controllability of Electric Loads," *Proceedings of the IEEE*, vol. 99, pp. 184-199, 2011.
- [4] E. M. Davidson, S. D. J. McArthur, M. J. Dolan, and J. R. McDonald, "Exploiting intelligent systems techniques within an autonomous regional active network management system," in *Power & Energy Society General Meeting, 2009. PES '09. IEEE*, 2009, pp. 1-8.
- [5] E. M. Davidson, M. J. Dolan, S. D. J. McArthur, and G. W. Ault, "The Use of Constraint Programming for the Autonomous Management of Power Flows," in *Intelligent System Applications to Power Systems, 2009. ISAP '09. 15th International Conference on*, 2009, pp. 1-7.
- [6] I. Richardson, M. Thomson, D. Infield, and C. Clifford, "Domestic electricity use: A high-resolution energy demand model," *Energy and Buildings*, vol. 42, pp. 1878-1887, 2010.
- [7] A. Fazeli, Johnson, C M, Sumner, M, Christopher, E, "A NOVEL STOCHASTIC MODELLING APPROACH FOR ELECTRIC VEHICLE CHARGING POWER AND ENERGY REQUIREMENTS " presented at the Innovative smart grid technologies, Washington DC, 2014.
- [8] A. Fazeli, Sumner, M, Johnson, C M, Christopher, E,, "Coordinated Optimal Dispatch of Distributed Energy Resources within a Smart Energy Community Cell," presented at the 2012 3rd IEEE PES Innovative Smart Grid Technologies Europe Berlin, 2012.
- [9] A. W. M. J. v. S. a. M. H. M. d. Wit, "ADVANCED SIMULATION OF BUILDING SYSTEMS AND CONTROL WITH SIMULINK," presented at the Eighth International IBPSA Conference, 2003.
- [10] P. S. Anca D.Hansen, Lars H. Hansen and Henrik Bindner, "Models for a Stand-Alone PV System," Riso National Laboratory, Roskilde December 2000.
- [11] M. E. R. D. P. Hohm, "Comparative Study of Maximum Power Point Tracking Algorithms," *PROGRESS IN PHOTOVOLTAICS: RESEARCH AND APPLICATIONS*, vol. 11, pp. 47-62, 2003.
- [12] N. W. Miller, "Dynamic modeling of GE 1.5 and 3.6 MW wind turbine-generators for stability simulations," presented at the Power Engineering Society General Meeting, 2003, IEEE, 2003.
- [13] X. G. Qijun Deng, Hong Zhou and Wenshan Hu, "system modelling and optimization of microgrid using genetic algorithm," presented at the Intelligent Control and Information Processing (ICICIP), Dept. of Autom., Wuhan Univ., Wuhan, China 2011.
- [14] R. X. a. J. F. Hongwen He \*, "Evaluation of Lithium-Ion Battery Equivalent Circuit Models for State of Charge Estimation by an Experimental Approach," *Energies*, vol. 4, 2011.
- [15] MathWorks. (2014). *S-Function*. Available: <http://nl.mathworks.com/help/simulink/slref/sfunction.html>
- [16] NISSAN. (2012, 11/07/2013). *NISSAN LEAF*. Available: <http://www.nissanusa.com/electric-cars/leaf/versions-specs/>
- [17] Dimplex, Ed., *Dimplex heat pumps*. 2009, p.^pp. Pages.
- [18] T. E. ToolBox. *Thermal properties of water*. Available: [http://www.engineeringtoolbox.com/water-thermal-properties-d\\_162.html](http://www.engineeringtoolbox.com/water-thermal-properties-d_162.html)
- [19] A. Fazeli, M. Sumner, E. Christopher, and M. Johnson, "Power flow control for power and voltage management in future smart energy communities," in *Renewable Power Generation Conference (RPG 2014), 3rd*, 2014, pp. 1-6.
- [20] R., Davies, A Fazeli, SP Oe, M Sumner, M Johnson, E Christopher, "Energy Management Research using Emulators of Renewable Generation and Loads," presented at the Innovative Smart Grid Technologies (ISGT 2013), Washington DC, USA, 2012.